# NUMERICAL STUDY ON THE COMBUSTION PROCESS OF A BIOGAS SPARK IGNITION ENGINE

by

***Jose L. E. CARRERA [a*], Jose M. A. RIESCO [b], Simon M. MARTINEZ [c], Fausto A. C. SANCHEZ [c], and Armando M. GALLEGOS [b]***

[a] Universidad Politecnica de Zacatecas, Zacatecas, Mexico
[b] Universidad de Guanajuato, Guanajuato, Mexico
[c] Universidad Autonoma de Nuevo Leon, Nuevo Leon, Mexico

Original scientific paper
DOI: 10.2298/TSCI111115152C

*The fuel called biogas is obtained through anaerobic digestion of different types of organic waste, providing a way to tap the energy stored in organic matter. The use of this fuel is also attractive from the standpoint of global warming because its application does not register a net emission of carbon dioxide into the atmosphere. One possible use for this fuel is to feed the spark-ignition internal combustion engines. In the present, there is little information available about the process of combustion in internal combustion engines fueled by biogas. The combustion process of an internal combustion engine ignition powered by biogas is characterized in terms of the duration of combustion, i. e., depending on the time elapsed while the reactants (methane and oxygen) are transformed into products (mainly carbon dioxide and water). This study numerically evaluates the way in which the geometrical parameters such as the compression ratio and operating parameters like engine speed, the excess air, the time of spark timing and carbon dioxide content of biogas affect the evolution of the combustion process. To carry out this study, a five factors and two levels experiment was designed and conducted, based on which, the most influential parameters were identified. Equations expressing the combustion characteristic parameters, as a function of the geometric and operation parameters of a spark ignited engines, are delivered as a result.*

Key words: *biogas combustion, computational fluid dynamics, Wiebe function, spark ignition*

## Introduction

The spark ignited (SI) reciprocating internal combustion engines are devices widely used to produce power from chemical energy stored in a fuel, SI engine's size ranges from a few cubic centimeters of displacement, single cylinder, up to several liters of displacement and 16 cylinders per engine. Hydrocarbons, which are used to feed the SI engines, are expensive fuels, promises to be even more expensive in the future, at some point have to run out and contribute significantly to the problem of global warming. Biogas is a fuel that can be used to feed the SI engines. Moreover, biogas is a fuel that is derived from the anaerobic decomposition of organic matter, which includes sewage, municipal waste, feces of cattle and agricultural waste. As a product of the anaerobic decomposition of organic matter, a residue rich in minerals that can be used as fertilizer is obtained [1]. If the organic matter that can be used to produce biogas is not used in this way, it becomes a problem of contamination by bad odorsreleased in to the air; be-

* Corresponding author; e-mail: jlcarrera20@hotmail.com

sides, we can find methane within the gases released, which traps more radiation that $CO_2$, the main cause of global warming [2].

The use of biogas as fuel of engines can help to reduce oil use, also, a resource that is being wasted, making no net contribution to the $CO_2$ into the atmosphere will be used.

The adaptation of a fossil fuel powered SI engine to work with biogas can be done without major mechanical modifications [3-7]; however, it would be used an SI engine to work with a fuel for which it was not designed; therefore there is no guarantee that its performance is as good as it could be. The performance of the SI engines depends on many factors, of which the most important is the process of combustion, in terms of available energy that is lost in each process [8].

If we wish to simulate the operation of the engine using a thermodynamic model, it is also important to know the details of the combustion process. The simulations using the thermodynamic models are important because they allow the calculation of the size of an engine required, the preparation of the test and the development of the control system.

The combustion process of an internal combustion engine ignition can be characterized in terms of combustion duration, spark timing, and the completeness of the combustion. A parameter that somehow describes the evolution of the combustion process is also needed, as does the shape parameter of the Wiebe's function. To the present, there have been some studies on the performance and emissions of biogas-fed SI engines [9-13]; however, there is little information available about the combustion process.

For its characterization, the combustion process is typically divided into the following stages [8].

*Flame-development angle*: it is the crank angle interval between the spark discharge and the time when a small but significant fraction of the cylinder mass has burned or fuel chemical energy has been released. Usually this fraction is 10%, though other fractions such as 1 and 5 percent have been used. This angle is sometimes called ignition delay.

*Rapid-burning angle*: The crank angle interval required to burn the bulk of the charge. It is defined as the interval between the end of the flame-development stage and the end of the flame-propagation process (usually mass fraction burned or energy-release fraction of 90%). An alternative definition for this angle uses the maximum burning rate to define an angle or time characteristic of the bulk charge burning process [14].

Finally, the overall burning angle is defined as the duration of the overall burning process. It is the sum of the flame-development angle and the rapid burning angle.

Wiebe's equation [15] is widely accepted as a tool for describing the evolution of the combustion process in spark ignition engine. Wiebe's equation is:

$$x_b = 1 - \exp\left[-a\left(\frac{\theta - \theta_0}{\Delta\theta}\right)^{m+1}\right] \tag{1}$$

where $\theta$ is the crack angle, $\theta_0$ – the start of combustion, $\Delta\theta$ – the total combustion duration ($x_b$ = = 0 to $x_b \approx 1$), and $a$ and $m$ are adjustable parameters which fix the shape of the curve.

The value of $\theta_0$ can be taken as the position of the crankshaft angle at which the spark was ignited. The $a$ parameter defines the maximum fraction of the energy released or burned mass, a value of $a = 6908$ corresponds to a mass fraction burned of $x_{b,max.} = 0.999$.

Finally, the factor m changes the curve of evolution of combustion as shown in fig. 1.

In the present, information can be found about recommended values for the characterization of the combustion process with Wiebe's function in diesel and gasoline powered engines, but not for biogas fueled engines, this paper proposes a contribution in this regard by numerically characterizing the combustion process of a six-cylinder engine fed by biogas of different compositions.

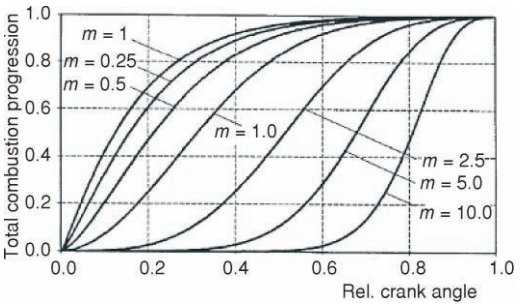


**Figure 1. Evolution of the combustion process with different values of shape parameter in Wiebe's equation [16]**

The combustion process of an SI engine depends strongly on the velocity field and the level of turbulence inside the combustion chamber at the time when the spark is ignited; it also depends on the pressure, temperature, and composition of the gas mixture inside the cylinder. The computational fluid dynamics (CFD) is a tool capable of calculating the parameters which depend on the combustion process and, therefore, the evolution of the combustion process. For this reason, this tool has been chosen in this work to characterize the combustion process.

## Methodology

### *Description of the experiment designed*

To carry out this work a five factors and two levels full factorial experiment was developed. The factors considered and their respective levels are shown in tab. 1, the nomenclature shown on this table is adopted for the rest of the work, for example, A+ means compression ratio of 14 and A– a compression ratio of 8.4. It is noteworthy that the compression ratio was changed by increasing the cylinder displacement at constant volume and shape of the combustion chamber.

**Table 1. Factors and factor levels used in the experiment**

| Factor | Variable name | High level | Low level |
|---|---|---|---|
| $r$ | A | 14 | 8.4 |
| $\omega$ [rpm] | B | 3000 | 1000 |
| $\varphi$ | C | 1.5 | 1 |
| $\theta_0$ [crack angle degree] | D | 0 | –40 |
| $\psi$ | E | 40 | 0 |

The factors considered were chosen because they directly influence the combustion process. The reasons why these factors affect the combustion process are detailed below:

*Compression ratio*. By increasing the compression ratio, reached temperature and pressure inside the cylinder also increase and, as already mentioned, the evolution of the combustion process depends on these factors.

*Crankshaft rotational speed*. The speed at which the piston moves obviously affects the velocity field inside the cylinder, which directly affects the combustion process.

*Relative air-fuel ratio and percentage of $CO_2$ in the fuel*. The composition of the gas mixture inside the cylinder is affected by these factors, which directly reflects on he evolution of the combustion process.

*Spark timing*. The conditions of pressure and temperature of the mixture of gases inside the cylinder affect the combustion process when the spark is ignited; therefore, the combustion process depends on when the spark is turned on.

### *Simulated engine and its geometry*

For the creation and meshing of the computational domain software GAMBIT® was used. The simulated engine characteristics are shown in tab. 2, while fig. 2 shows the modeled cylinder (a) and its combustion chamber (b). Figure 3 shows a detailed view of the combustion chamber, numbers 1 and 2 indicate the place where the intake and the exhaust valves are situated, respectively, and number 3 indicates the place where the spark plug enters.

**Table 2. Characteristics of the simulated engine**

| Number and arrangement of cylinders | V6 |
|---|---|
| Valves per cylinder | 2 |
| Aspiration | Natural |
| Bore | 87 mm |
| Stroke | 89 mm |
| Total displacement volume | 3.3 liters |
| Nominal power | 100 HP |

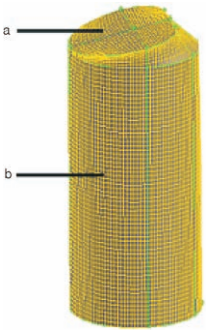


**Figure 2. Cylinder and combustion chamber modeled**

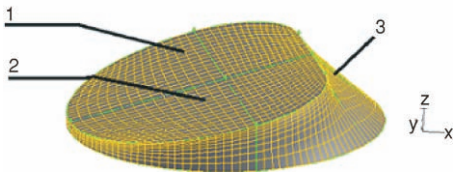


**Figure 3. Close up to the combustion chamber modeled**

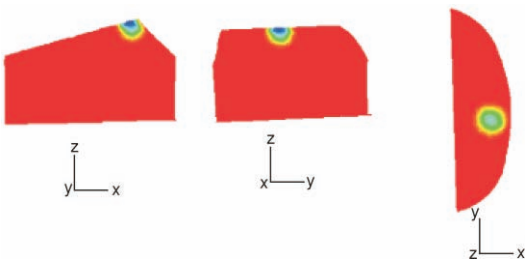


**Figure 4. Localization of the spark**

For a better understanding of the location of the spark, fig. 4 shows transversal cuts made to the cylinder in the point where the spark is located. The geometry has 64,000 hexagonal cells; it was decided to use this number of cells after performing a mesh sensitivity analysis, which worked with meshes of 10,500, 19,400, 35,000, 64,000, and 75,000 cells, getting identical results with the two geometries of more cells. It is noteworthy that increasing the number of cells should reduce the time step to avoid problems of convergence, so the step value had to be 0.25° of crankshaft rotation.

### *Description of the simulation*

The software FLUENT® which is based on the finite volume method, was used to run the simulations. The governing equations ap-

plied to the computational domain include the mass conservation eq. (2), momentum conservation eq. (3), energy equation eq. (4), equations of state eq. (5), one transport equation of form of eq. (6) for conservation of each species, the turbulence model $k$-$\omega$ eq. (7) and eq. (8), and the combustion model. The equations to be solved are shown in tab. 3. The $k$-$\omega$ turbulence model [17] was selected because it was the one that provided the best agreement with the results published by Porpatham *et al.* [12]. The selected combustion model is the Eddy dissipation concept [18], which is an extension of the Eddy dissipation model that assumes that the combustion process is governed by the turbulent transport of the flame front inside the cylinder, but allows the incorporation of chemical kinetic mechanisms that allow including CO within the combustion products. According to the way it the combustion process is described in the reading, turbulent flame propagation is the mechanism that governs this process [8]; therefore, the Eddy dissipation concept model seems appropriate for the simulations. This model assumes that reaction occurs in small turbulent structures, called the fine scales. The length fraction of the fine scales is modeled as shown by eq. (9), The volume fraction of the fine scales is calculated as $\xi^{*3}$ Species are assumed to react in the fine structures over a time scale which is calculated according to eq.

**Table 3. Set of partial differential equations to be solved and combustion model**

| | | |
|---|---|---|
| Mass conservation | $\frac{\partial p}{\partial t} + \mathrm{div}(\rho u) = 0$ | (2) |
| x-momentum | $\frac{\partial(\rho u)}{\partial t} + \mathrm{div}(\rho u\vec{\mathrm{u}}) = -\frac{\partial p}{\partial x} + \mathrm{div}(\mu \mathrm{grad} u) + S_{\mathrm{Mx}}$ | (3a) |
| y-momentum | $\frac{\partial(\rho v)}{\partial t} + \mathrm{div}(\rho v\vec{\mathrm{u}}) = -\frac{\partial p}{\partial y} + \mathrm{div}(\mu \mathrm{grad} v) + S_{\mathrm{My}}$ | (3b) |
| z-momentum | $\frac{\partial(\rho w)}{\partial t} + \mathrm{div}(\rho w\vec{\mathrm{u}}) = -\frac{\partial p}{\partial z} + \mathrm{div}(\mu \mathrm{grad} w) + S_{\mathrm{Mz}}$ | (3c) |
| Energy equation | $\frac{\partial(\rho i)}{\partial t} + \mathrm{div}(\rho i\vec{\mathrm{u}}) = -p\mathrm{div}\vec{u} + \mathrm{div}(K\mathrm{grad}T) + \Phi + S_i$ | (4) |
| State equations | $p = \rho \mathrm{R} T$<br>$i = C_{\mathrm{V}} T$ | (5a)<br>(5b) |
| Species conservation and transport | $\frac{\partial(\rho\phi_i)}{\partial t} + \mathrm{div}(\rho\phi_i\vec{\mathrm{u}}) = \mathrm{div}(\Gamma \mathrm{grad}\phi_i) + S_{\phi_i}$ | (6) |
| Turbulence model | $\frac{\partial}{\partial t}(\rho k) + \mathrm{div}(\rho k u_i) = \mathrm{div}(\Gamma_\kappa \mathrm{grad} k) + G_{\mathrm{k}} - Y_{\mathrm{k}} + S_{\mathrm{k}}$<br>$\frac{\partial}{\partial t}(\rho\omega) + \mathrm{div}(\rho\omega u_i) = \mathrm{div}(\Gamma_\omega \mathrm{grad}\omega) + G_\omega - Y_\omega + S_\omega$ | (7)<br>(8) |
| Combustion model | $\xi^* = C_\xi \sqrt[4]{\frac{\upsilon\varepsilon}{k}}$<br>$\tau^* = C_\tau \sqrt{\frac{\upsilon}{\varepsilon}}$<br>$S_i = \frac{\rho\xi^{*2}}{\tau^*(1-\xi^{*3})}(Y_i^* - Y_i)$ | (9)<br>(10)<br>(11) |

(10). The source term in the conservation equation for the mean species *i*, eq. (6), is modeled as shown in eq. (11).

A two-step and three reactions mechanism which allows the calculation of the amount of CO that is generated during the combustion of methane in the SI engine modeled was used for the simulations. The reactions considered are the following.

$$CH_4 + 1.5O_2 \rightarrow CO + 2H_2O \tag{12}$$

$$CO + ½O_2 \rightarrow CO_2 \tag{13}$$

$$CO_2 \rightarrow CO + ½O_2 \tag{14}$$

Reaction of eq. (12) describes the oxidation of methane to form CO and water, reaction of eq. (13) shows the formation of $CO_2$ while the reaction of eq. (14) considers the dissociation reaction of the latter specie.

### *Initial and boundary conditions*

In order to take in consideration the effect that the exhaust gases have in the composition of the charge inside the cylinder at the beginning of the compression stroke, the initial conditions used in the simulation were calculated from a thermodynamic model for SI engines [19], which considers the residual gas fraction.

The pressure and temperature conditions at the beginning of the compression stroke, as well as the composition of the gas mixture inside the cylinder at the moment are particularly dependent on compression ratio, excess air, and $CO_2$ content of the biogas, considering that there are two levels of each of these variables, only 8 different boundary conditions in the 32 different case studies were used.

The boundary conditions are shown in tab. 4, while tab. 5 shows when each of the 8 initial conditions are used. As boundary conditions, the no-slip condition on the walls and the temperature were used. A constant temperature of 400 K was used even knowing that the temperature of the cylinder walls varies spatially and temporally, since this variation of temperature affects very little to the properties of the mixture of gases inside the cylinder [20].

**Table 4. Initial conditions**

| No. | $T$ [K] | $p$ [kPa] | $YO_2$ | $YCH_4$ | $YCO_2$ | $YH_2O$ |
|---|---|---|---|---|---|---|
| 1 | 321 | 104 | 0.2103 | 0.0347 | 0.0456 | 0.0043 |
| 2 | 305 | 99 | 0.2191 | 0.0361 | 0.0056 | 0.0043 |
| 3 | 341 | 110 | 0.2021 | 0.0505 | 0.0637 | 0.0047 |
| 4 | 308 | 100 | 0.2144 | 0.0563 | 0.0062 | 0.0051 |
| 5 | 330 | 104 | 0.2079 | 0.0341 | 0.0485 | 0.0063 |
| 6 | 310 | 97 | 0.2176 | 0.0356 | 0.0082 | 0.0066 |
| 7 | 358 | 111 | 0.1966 | 0.0499 | 0.0667 | 0.0069 |
| 8 | 317 | 98 | 0.2128 | 0.0529 | 0.0090 | 0.00742 |

**Table 5. Description of the cases shown in tab. 4**

| Case number | Compression | Air-fuel equivalent ratio | $CO_2$ content [%] |
|---|---|---|---|
| 1 | 14 | 1.5 | 40 |
| 2 | 14 | 1.5 | 0 |
| 3 | 14 | 1 | 40 |
| 4 | 14 | 1 | 0 |
| 5 | 8.4 | 1.5 | 40 |
| 6 | 8.4 | 1.5 | 0 |
| 7 | 8.4 | 1 | 40 |
| 8 | 8.4 | 1 | 0 |

The simulation results include the values of properties such as pressure, volume, temperature, and mass fraction of each species, with this information, the fraction of fuel burned can be calculated as:

$$x_b = \frac{y_{CH4.0} - y_{CH_4}}{y_{CH4.0}} \tag{15}$$

where $x_b$ is also known as fraction of heat released.

## Results and discussion

### *Combustion duration*

Figure 5 shows four lines of heat release. The four curves have the same compression ratio, the same engine speed and the same air-fuel equivalence ratio, two lines have the same spark timing and two lines have the same $CO_2$ content in the fuel.

It can be seen that the curves of heat release whose beginning is 40 degrees before top dead center (TDC) are in the beginning of pending higher than those starting at the TDC; however, the slope grows faster in the curves that began first resulting in a faster evolution of the combustion when it starts 40 degrees before TDC when it is initiated in the TDC.

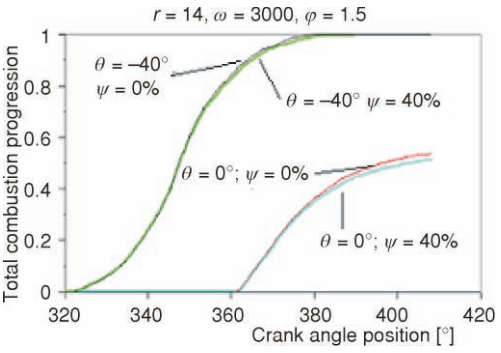


**Figure 5. Effect of ignition timing and percentage of $CO_2$ in the biogas in the release of heat**

It is also shown in fig. 4 that the different content of $CO_2$ in fuel does not cause that he heat release curves are significantly different.

For heat release curves in which the spark timing coincides with TDC, it is observed that almost half of the fuel remains unburned. For these curves, to define the combustion duration as the time between the spark timing crank angle and the 99% fuel consumed crank angle is meaningless since it would lead us to infinite combustion duration. For this reason, it was

adopted an alternative definition for the combustion duration based on the heat release rate (the time derivative of $x_b$), in which the end of the combustion process is defined when the derivative of the fraction of heat released ($dx/d\theta$) reaches a value of $1 \cdot 10^{-3}$ per degree, this value coincides with a value around 0.99 for $x_b$ when most of the fuel is burned.

Figure 6 shows the average effect that each of the variables has in the combustion duration. Each point of those who plotted in this figure represents the average value of 16 numerical experiments. The graph shows 5 lines of different slope, so the first line on the left states that the average value of the combustion duration was 35 degree of crankshaft rotation when the compression ratio used was 14, and when the compression ratio used was 8.4 the average value of the combustion duration was 48 degrees of crankshaft rotation. This indicates that the greater is the compression ratio the lower the combustion duration; this is because by increasing the compression ratio increases the pressure and temperature inside the cylinder charge, which facilitates the propagation of the flame front.

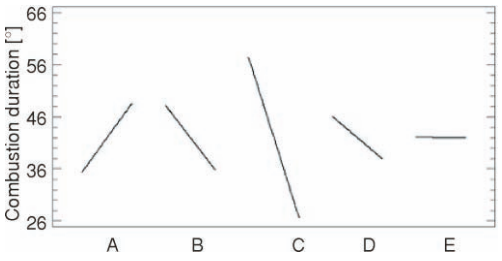


**Figure 6. Main effects of the variables studied in the combustion duration**

The second line of fig. 6 shows the effect of engine speed on the duration of combustion, it is observed that to increase the engine speed also increases combustion duration. This result was expected since the duration of combustion is measured in degrees of crankshaft rotation, and when the engine speed increases every degree of crankshaft rotation takes less time to spend.

The third line shows that the combustion duration is lower when the air-fuel ratio is stoichiometric than when lean mixtures are used, which is due to the degree of dilution of the mixture of gases inside the cylinder.

The fourth line of fig. 6 shows that advance the start of combustion decreases the duration of combustion. If combustion starts before the cylinder reaches TDC, the cylinder pushes the fresh gases toward the front flame, increasing the rate at which gases are burned and reducing the duration of combustion. On the other hand, if the combustion starts when the piston is at TDC, then the flame front and the fresh gas move in the same direction, decreasing the rate at which reactants are consumed and increases the duration of the combustion.

Finally, the fifth line of fig. 6 shows the effect of the $CO_2$ content of the fuel in the combustion duration. It can be seen first, that this effect is the smallest of all those considered in this study. It also shows that, on average, the duration of combustion increases with increasing $CO_2$ content of the fuel. A multiple factor regression analysis was carried out to describe the relationship between the duration of combustion and the five variables studied. The equation of the fitted model is:

$$\Delta\theta_c = 42.0 - 6.625x_1 + 6.25x_2 + 15.375x_3 + 4.0625x_4 + 0.0625x_5 \tag{16}$$

where $x_1, x_2, x_3, x_4$, and $x_5$ are the coded variables for the compression ratio, engine speed air-fuel equivalence ratio, and the spark timing and can take values from 1 to –1, according to the equations:

$$x_1 = \frac{r}{2.8} - 4 \tag{17}$$

$$x_2 = 0.001\omega - 2 \tag{18}$$

$$x_3 = 4\phi - 5 \tag{19}$$

$$x_4 = 0.05\theta_0 + 1 \tag{20}$$

$$x_5 = 0.05\psi - 1 \tag{21}$$

Equation (16) calculates the duration of combustion of the cases studied with an average absolute error of 8.789 degree of crankshaft rotation.

The interactions between the variables studied could also influence significantly the combustion duration. To evaluate this possibility the Pareto chart of the fig. 7 is used, this figure shows, in descending order, the standardized effect that each variable and interaction between the variables have in the combustion duration.

According to what is observed in fig. 7 the air-fuel equivalence ratio is the most influential factor, followed by the compression ratio and the engine speed. After these variables, the interaction between engine speed and the spark timing appear as the interaction that influences the most the combustion duration, but with an effect that is smaller than that of the three variables mentioned above.

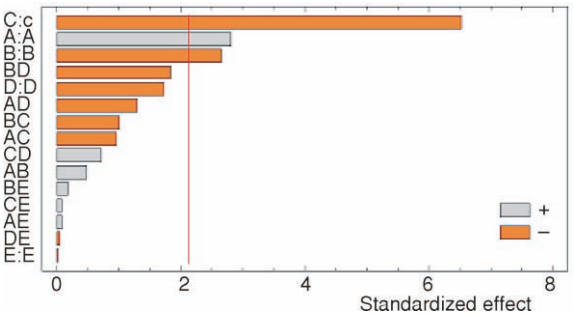


**Figure 7. Pareto chart for the combustion duration**

Based on what is observed in figs. 6 and 7, a multiple factor regression analysis was carried out to describe the relationship between the duration of combustion and the five largest standardized effect parameters. The equation of the fitted model is:

$$\Delta\theta_c = 42 + 15.375x_3 + 6.625x_1 + 6.25x_2 - 4.313x_2x_4 + 4.0625x_4 \tag{22}$$

Equation (22) calculates the duration of combustion of the cases studied with an average absolute error of 8.18 degrees of crankshaft rotation.

### *Combustion completeness parameter*

The $a$ parameter is related to the final amount of fuel burned by the equation:

$$a = -\ln(1 - x_{b,max.}) \tag{23}$$

Figure 8 shows the main effects of each of the variables studied in the parameter $a$. This figure shows that as the compression ratio increases also the value of parameter $a$ increases, and; therefore, the final value of the fraction of fuel burned. It is also seen that increasing the engine speed the value of parameter $a$ decreases, which means that more fuel is not burned. With respect to increasing in air-fuel equivalence ratio, it is observed that the higher this is, the smaller the parameter $a$, this is because the flame front spreads more

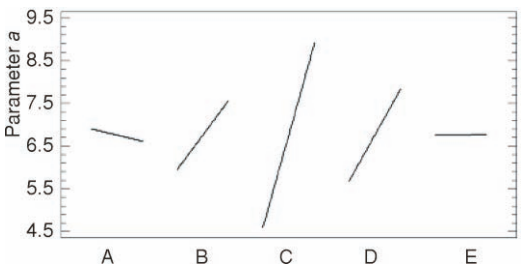


**Figure 8. Main effects in the parameter *a***

difficulty in the more dilute mixtures, which leads to more unburned fuel. The same effect can be observed in the presence of carbon dioxide from the fuel, although to a lesser degree.

Finally, it is observed that when the spark is ignited at TDC, the values obtained of the parameter *a* are lower than those obtained when the spark is ignited before TDC, which is obviously due to the available time to carry out the combustion and to the interval of time when flame front and the cylinder move toward each other. A regression analysis was performed for the parameter *a* taking in consideration the compression ratio, engine speed, air-fuel equivalence ratio, spark timing, and $CO_2$ content as independent variables. The equation of the fitted model is:

$$a = 6.76 + 0.144x_1 - 0.813x_2 - 2.167x_3 - 1.078x_4 - 0.0091x_5 \quad (24)$$

Equation (24) calculates the values of the experiment performed with an average absolute error of 1.817.

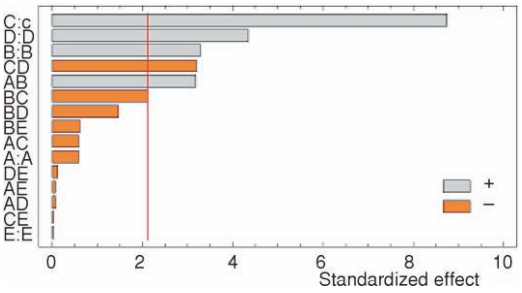


**Figure 9. Pareto diagram for the parameter *a***

Figure 9 shows the Pareto chart for the parameter *a*. This figure shows that the most influential parameters and interactions in the value of the parameter *a*, which is representative of the completeness of combustion, are: air-fuel equivalent ratio, spark timing, engine speed, the interaction between the air-fuel equivalence ratio and the spark timing, the interaction between the compression ratio and the engine speed, and the interaction between the engine speed and the air-fuel equivalence ratio. Based on this information these parameters are chosen to be part of the regression analysis for the parameter *a*. The equation of the fitted model is:

$$a = 6.755 - 2.167x_3 - 1.078x_4 - 0.813x_3 - 0.79x_3x_4 + 0.788x_1x_2 \quad (25)$$

Equation (25) calculates the values of the experiment performed with an average absolute error of 0.962.

### *Form factor of the Wiebe function*

Once the values of the duration and completeness of combustion have been identified as described above, we only need to identify the shape parameter of the Wiebe function that allows for the best fit to the heat release curve obtained originally; in other words, the value of the form factor chosen is the one that minimizes the absolute error between the original and the adjusted curves, which is defined as:

$$error = \int_{\theta_0}^{\theta_f} abs(x_{b,exp.} - x_{b,Wiebe})d\theta \quad (26)$$

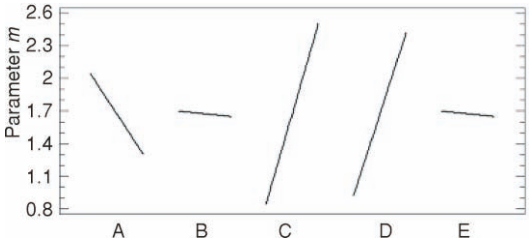


**Figure 10. Main effects on the form factor *m***

Figure 10 shows how the parameters considered in this study affect the value of the parameter *m* that best fits the curve of heat release.

We can see in fig. 10 that increasing values of compression ratio, engine speed, and content of biogas increases the value of the parameter *m* that best fits the original curve of heat release; in other words, the curve has a form of "s" increasingly pronounced. It is also shown in this figure that increasing the air – fuel equivalence ratio and the spark timing makes the heat release curve has a profile of "s" less pronounced. A regression analysis for the form factor *m*, with the five parameters of the fig. 10 as independent variables gives the next equation:

$$m = 1.675 + 0.368x_1 - 0.25x_2 - 0.8321x_3 - 0.75x_4 + 0.025x_5 \quad (27)$$

Figure 11 shows the Pareto chart for the form factor. This Figure shows that the factors that most strongly influence the parameter *m* are: air-fuel equivalence ratio, spark timing, compression ratio, interaction between compression ratio and engine speed and interaction between engine speed, and the spark timing. These parameters are selected to be part of the model for the parameter *m*, which appears below:

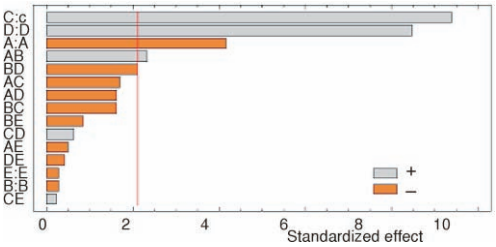


**Figure 11. Pareto chart for the form factor of the Wiebe's function**

$$m = 1.675 - 0831x_3 - 075x_4 + \\ + 0.369x_1 + 0.206x_1x_2 - 0.188x_2x_4 \quad (28)$$

Using eq. (28) gives a mean absolute error of 0.363 when compared with values obtained from the original fit of the parameter *m*, while using eq. (27) gives a mean absolute error of 0.4328.

Figure 12 shows the curve fit of a fraction of heat released as an example of how the equations proposed in this paper fit the original curves, in this case the shape parameter value that best fits the original curve is 4.9.

Figure 13 shows the variation of the combustion duration with the equivalence ratio obtained by Porpatham *et al*. [12] and fig. 14 shows the same variation but calculated by means of the equations presented in this paper, using the parameters specified in fig. 13. There is a good agreement between the experimental data and the values predicted by the equations presented in

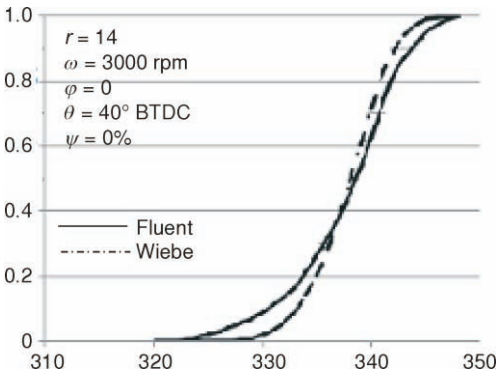


**Figure 12. Original curve of fraction of heat released and Wiebe's function fitted curve**

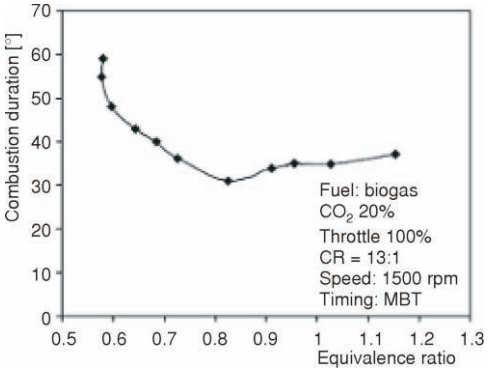


**Figure 13. Experimental variation of the combustion duration as function of the equivalence ratio [12]**

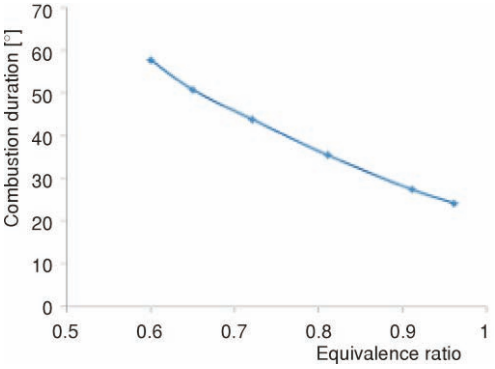


**Figure 14. Variation of the combustion duration as function of the equivalence ratio calculated by means of eq. (22)**

this paper, however the differences than can be observed can be due to the different combustion chambers of the cylinders used in the experimental study and this numerical study.

*Flame propagation*

Figure 15 shows the contours of mass fraction of $CH_4$, drawn in a cut of the cylinder, made at the point where the spark is located on a plane perpendicular to the "y" co-ordinate axis. Red color indicates that there is a fresh mixture of air and fuel. Blue color indicates that there is no more fuel, no more $CH_4$. The thin, yellow and green zone is the flame front, in this way, fig. 15 shows the flame propagation inside the cylinder in different moments. It can be seen that the flame propagation is almost spherical which is in agreement with the results presented by Yasar [21], Zhichao and Reitz [22], and Dinler and Yucel [23].

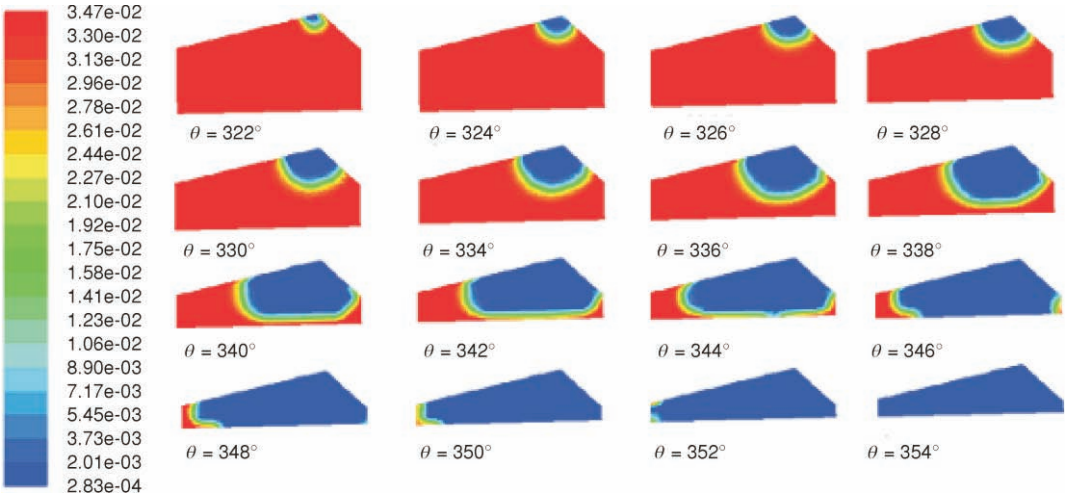


**Figure 15. Contours of mass fraction of $CH_4$ at different instants**
(for color image see journal web site)

## Conclusions

In this paper, a CFD model of a biogas fueled SI engine was developed. This model is able to calculate the speed at which the fresh gas mixture inside the cylinder is converted in burned gases.

From the factors considered in this paper, the most important for the combustion process was that experiments were carried out that allow the evaluation of the effect that the compression ratio, engine speed air-fuel equivalence ratio, spark timing, and biogas content have in the combustion process, characterized by the combustion duration, combustion completeness, and the form factor.

The spark timing is another factor that shows to be very important for the development of the combustion process. If the spark is not turned on soon enough, there will not be enough time to burn all the fuel. When the engine is fed on poor fuel-air mixtures, the spark timing advance needs to be the greatest, this is because the flame propagation is the hardest under this conditions.

The $CO_2$ content of the fuel is, from the factors considered in the study, the one that has less influence on the combustion process. The effect of this parameter is very poor because the main diluent of the fuel-air mixture is the nitrogen. At the light of this, it is not considered to be necessary to extract the $CO_2$ from the biogas for its use on alternative internal combustion engines.

Relationships were found for the duration of combustion, the completeness of combustion and the shape parameter depending on the studied variables that most strongly influence the combustion process.

The found equations allow the calculation of the combustion process evolution by means of a Wiebe burning law; this way, thermodynamic one-zone simulation can be carried out with the next advantages.

- There is no need for the user to have experience in using the Wiebe burning law.
- The combustion process is calculated taking into consideration the compression ratio, engine speed, air-fuel ratio, spark timing, and $CO_2$ content of the fuel.
- The thermodynamic models take a lot of less time to be calculated than the multidimensional ones.
- More investigation is needed in order to quantify the effect of the shape of the combustion chamber in the combustion process.

## Nomenclature

$a$ – completeness parameter, [–]
$C_V$ – constant volume specific heat, [kJkg$^{-1}$K$^{-1}$]
$G_k$ – generation of turbulence kinetic energy due to mean velocity gradients
$G_\omega$ – generation of specific dissipation rate
$i$ – specific internal energy, [kJkg$^{-1}$]
$K$ – thermal conductivity, [Wm$^{-1}$K$^{-1}$]
$k$ – turbulent kinetic energy
$m$ – form factor, [–]
$p$ – pressure, [kPa]
R – gas constant, [kJkg$^{-1}$K$^{-1}$]
$r$ – compression ratio [–]
$S$ – source term
$T$ – temperature, [K]
$t$ – time, [s]
$u$ – velocity component in the x-direction, [ms$^{-1}$]
$\vec{u}$ – vector velocity, [ms$^{-1}$]
$v$ – velocity component in the y-direction, [ms$^{-1}$]
$w$ – velocity component in the z-direction, [ms$^{-1}$]
$x$ – coded variable, [–]
$x, y, z$ – spatial co-ordinates, [m]
$x_b$ – mass fraction burned
$Y$ – mass fraction, [–]
$Y^*$ – the fine-scale species mass fraction after reacting over the time $\tau^*$, [–]

### *Greek symbols*

$\Gamma$ – effective diffusivity, [m$^2$s$^{-1}$]
$\Delta\theta_c$ – combustion duration, [°]
$\theta$ – crank angle position, [°]
$\mu$ – viscosity, [kgm$^{-1}$s$^{-1}$]
$\xi$ – fine scale, [–]
$\rho$ – density, [kgm$^{-3}$]
$\tau$ – time scale, [–]
$\upsilon$ – kinematics viscosity, [m$^2$s$^{-1}$]
$\Phi$ – internal energy generated due to viscous stress
$\phi$ – scalar property
$\varphi$ – air-fuel equivalence ratio
$\psi$ – $CO_2$ content in biogas
$\omega$ – engine speed [rpm], specific dissipation rate, [s$^{-1}$]

### *Acronyms*

BTDC – before top dead center
TDC – top dead center
SI – spark ignition

## References

[1] Houdkova, L., *et al*., Biogas – A Renewable Source of Energy, *Thermal Science, 12* (2008), 4, pp. 27-33
[2] Bond, T., *et al.*, Global Atmospheric Impacts of Residential Fuels, *Energy for Sustainable Development, 8* (2004), 3l, pp. 20-32
[3] Pipatmanomai, S., *et al*., Economic Assessment of Biogas-to-Electricity Generation System with H2S Removal by Activated Carbon in Small Pig Farm, *Applied Energy, 86* (2009), 5, pp. 669-674
[4] Jawurek, H. H., *et al.*, Biogas/Petrol Dual Fuelling of SI Engine for Rural Third World Use, *Biomass, 13* (1987), 2, pp. 87-103
[5] Kanaiyalal, B., Development of a Single Cylinder SI Engine for 100% Biogas Operation, M. Sc. thesis, Indian Institute of Science, Bangalore, India, 2006
[6] Mueller, G. P., Landfill Gas Application Development of the Caterpillar G3600 Spark-Ignited Gas Engine, *J. Eng. Gas Turbines Power, 117* (1995), 4, pp. 820-826
[7] Tippayawong, N., *et al.*, Long-Term Operation of a Small Biogas/Diesel Dual-Fuel Engine for On-Farm Electricity Generation, *Biosystems Engineering, 98* (2007), 1, pp 26-32
[8] Heywood, J. B., Internal Combustion Engine Fundamentals, McGraw-Hill, New York, USA, 1988
[9] Raine, Z., *et al*., Comparison of Emissions from Natural Gas and Gasoline Fuelled Engines – Total Hydrocarbon and Methane Emissions and Exhaust Gas Recirculation Effects, SAE paper 970743, 1997
[10] Vianna, S., *et al*., Study of the Effects of Intake Temperature on the Performance of Turbocharged Gas – Powered Engines, SAE paper 921494, 1992
[11] Jingdang, H., Crookes, R. J., Assessment of Simulated Biogas as a Fuel for the Spark Ignition Engine, *Fuel, 77* (1998), 15, pp. 1793-1801
[12] Porpatham, E., *et al*., Investigation on the Effect of Concentration of Methane in Biogas when Used as a Fuel for a Spark Ignition Engine, *Fuel, 87* (2009), 8, pp. 1651-1659
[13] Huang, J., Crookes, R. J., Spark-Ignition Engine Performance with Simulated Biogas: A Comparison with Gasoline and Natural Gas, *Fuel and Energy Abstracts, 40* (1999), 4, pp. 283-289
[14] Beretta, G. P., *et al*., Turbulent Flame Propagation and Combustion in Spark Ignition Engines, *Combust. Flame, 53* (1983), 3, pp. 217-245.
[15] Klein, M., Single-Zone Cylinder Pressure Modeling and Estimation for Heat Release Analysis of SI Engines Liu-Tryck, Linkopink, Sweden, 2007
[16] Merker, G. P., *et al*., Simulation of Combustion and Pollutant Formation for Engine-Development, Springer-Verlag, Berlin, 2006
[17] Wilcox, D. C., Turbulence Modeling for CFD. DCW Industries, Inc., La Canada, Cal., USA, 1998
[18] Gran, I. R., Magnussen, B. F., A Numerical Study of a Bluff-Body Stabilized Diffusion Flame, Part 2. Influence of Combustion Modeling and Finite-Rate Chemistry, *Combustion Science and Technology, 119* (1996), 1-6, pp. 191-217
[19] Carrera, J. L., Ideal and Air-Fuel Simulation of Internal Combustion Engines trough Burning Laws (in Spanish), M. Sc. thesis, Universidad de Guanajuato, Guanajuato, Mexico, 2007
[20] Jafari, A., Kazemzadeh, S., Effect of Fuel and Engine Operational Characteristics on the Heat Loss from Combustion Chamber Surfaces of SI Engines, *International Communications in Heat and Mass Transfer, 33* (2006),1, pp. 122-134
[21] Yasar, O., A New Ignition Model for Spark Ignition Simulations, *Parallel Computing, 27* (2001), 1 pp. 179-200
[22] Zhichao, T., Reitz, R., An Ignition and Combustion Model Based on the Level-Set Method for Spark Ignition Engine Multidimensional Modeling, *Combustion and Flame, 145* (2006), 1, pp. 1-15
[23] Dinler, N., Yucel, N., Combustion Simulation in a Spark Ignition Engine Cylinder: Effects of Air-Fuel Ratio on the Combustion Duration, *Thermal science, 14* (2010), 4, pp. 1001-1012

Paper submitted: November 15, 2011
Paper revised; June 13, 2012
Paper accepted:July 21, 2012